



ACADEMIC
PRESS

Available online at www.sciencedirect.com

SCIENCE @ DIRECT®

Journal of Solid State Chemistry 172 (2003) 296–304

JOURNAL OF
SOLID STATE
CHEMISTRY

<http://elsevier.com/locate/jssc>

Conductivity and carrier traps in $\text{La}_{1-x}\text{Sr}_x\text{Co}_{1-z}\text{Mn}_z\text{O}_{3-\delta}$ ($x = 0.3$; $z = 0$ and 0.25)

V.L. Kozhevnikov,^{a,*} I.A. Leonidov,^a E.B. Mitberg,^a M.V. Patrakeev,^a
A.N. Petrov,^b and K.R. Poeppelmeier^c

^a*Institute of Solid State Chemistry, Ural Division of RAS, Pervomaiskaya 91, GSP-145, Ekaterinburg 620219, Russia*

^b*Department of Chemistry, Ural State University, Kuibysheva 48, Ekaterinburg 620083, Russia*

^c*Department of Chemistry, Northwestern University, 2145 Sheridan Road, Evanston, IL 60208, USA*

Received 9 May 2002; received in revised form 27 August 2002; accepted 9 February 2003

Abstract

Measurements of the equilibrium oxygen content, electrical conductivity and thermopower in the perovskite-like solid solution $\text{La}_{0.7}\text{Sr}_{0.3}\text{Co}_{1-z}\text{Mn}_z\text{O}_{3-\delta}$ ($z = 0$ and 0.25) as a function of the temperature and oxygen partial pressure are used to determine the temperature dependence of the conductivity and thermopower at different values of the oxygen deficiency. A model for a hopping conductor with screened charge disproportionation is applied for the data analysis in combination with trapping reactions of n- and p-type carriers on local oxygen vacancy clusters and manganese cations, respectively. Changes in the ratio of n-type to p-type mobility are due to variations in oxygen vacancy concentration and manganese content, while the energetic parameters governing charge disproportionation of the trivalent cobalt cations and formation of vacancy associates are shown to be essentially invariable. These calculated charge carrier site occupancies are used to model temperature variations of the electrical properties in $\text{La}_{0.7}\text{Sr}_{0.3}\text{Co}_{1-z}\text{Mn}_z\text{O}_{3-\delta}$ in favorable correspondence with experimental observations.

© 2003 Elsevier Science (USA). All rights reserved.

Keywords: Perovskite; Cobaltite; Manganite; Oxygen content; Electrical conductivity; Thermopower; Hopping conductor

1. Introduction

The high-temperature chemistry and thermodynamics of co-substituted cobaltites $\text{La}_{1-x}\text{A}_x\text{Co}_{1-z}\text{B}_z\text{O}_{3-\delta}$, where *A* is an alkaline-earth metal and *B* is Mn, Cr, Fe or Ni, have been subjects of a number of studies. Attempts to interpret the electronic and oxygen ion transport properties have involved various conduction mechanisms and a variety of defect species. The most successful model developed by Sehlin et al. [1], which enabled the authors to describe the conductivity and thermopower in $\text{La}_{1-x}\text{Ca}_x\text{CoO}_3$ ($x = 0, 0.1, 0.2$) over the wide temperature range between 200 and 1500 K, is based on a small polaron conduction mechanism and screened charge disproportionation of Co^{3+} ions. Charge disproportionation involves the transfer of an electron between adjacent Co^{3+} ions, resulting in a population of Co^{2+} and Co^{4+} ions. Sites consisting of Co^{2+} or Co^{4+}

ions and the associated lattice distortion are occupied by a n- or p-type polaron, respectively. The screening interaction takes into account the influence of the valences of neighboring cobalt cations upon the free energy change associated with charge disproportionation. In the study [1] the calculated values of the thermopower in $\text{La}_{1-x}\text{Ca}_x\text{CoO}_{3-\delta}$ are somewhat smaller than the experimental data at high temperatures. This divergence can be related to the influence of oxygen vacancies that are known to form in the oxide in response to the intensive heating [2]. This supposition is corroborated by experimental findings in the work of Mizusaki et al. [3] where remarkable changes in the conducting properties of $\text{La}_{1-x}\text{Sr}_x\text{CoO}_{3-\delta}$ with oxygen non-stoichiometry were reported in the temperature range 600–1200 K. Because the oxygen partial enthalpy is smaller in $\text{La}_{1-x}\text{Ca}_x\text{CoO}_{3-\delta}$ compared to $\text{La}_{1-x}\text{Sr}_x\text{CoO}_{3-\delta}$ [2,4,5], the strontium-doped cobaltite is able to lose more oxygen at elevated temperatures than the calcium-doped material. Hence, the influence of the oxygen vacancies on the transport characteristics

*Corresponding author. Fax: +7-3432-71-00-03.

E-mail address: kozhevnikov@imp.uran.ru (V.L. Kozhevnikov).

will be more pronounced and thus more easily observable when strontium partially replaces lanthanum. Once oxygen vacancies form, either as point defects or associates [6,7], they affect the equilibrium of charged cobalt species and, thus, must be taken into account in model calculations. A straightforward way to examine the influence of the vacancies on the transport is to analyze the electronic properties at fixed values of the oxygen non-stoichiometry. However, it is simpler to measure changes in the properties when the oxygen partial pressure is varied at a given temperature. Therefore, the interrelation between oxygen content, oxygen partial pressure and temperature must be known for the analysis.

In the present study, the extent of oxygen non-stoichiometry δ , the electrical conductivity σ , and thermopower S are measured in the strontium-doped cobaltite $\text{La}_{0.7}\text{Sr}_{0.3}\text{CoO}_{3-\delta}$ as a function of temperature, T , and oxygen partial pressure, $p\text{O}_2$. The respective data are combined and used to analyze the temperature behavior of the thermopower at fixed values of oxygen content within the model developed by Sehlin et al. [1] for $\text{La}_{1-x}\text{Ca}_x\text{CoO}_3$ ($x = 0, 0.1, 0.2$). The original approach is extended to include the influence of oxygen vacancies on charge disproportionation and is incorporated in the calculations through consideration of the equilibrium of isolated and associated vacancies. More importantly, the modified model is employed to analyze the electron transport properties in $\text{La}_{0.7}\text{Sr}_{0.3}\text{Co}_{0.75}\text{Mn}_{0.25}\text{O}_{3-\delta}$. It is shown that the peculiarities in the high-temperature behavior of thermopower and conductivity in $\text{La}_{0.7}\text{Sr}_{0.3}\text{CoO}_{3-\delta}$ and $\text{La}_{0.7}\text{Sr}_{0.3}\text{Co}_{0.75}\text{Mn}_{0.25}\text{O}_{3-\delta}$ can be explained as due to an interplay of charge disproportionation and charge carrier trapping reactions.

2. Experimental

$\text{La}_{1-x}\text{Sr}_x\text{Co}_{1-z}\text{Mn}_z\text{O}_{3-\delta}$ ($x = 0.3$; $z = 0, 0.25$) powders were prepared using a standard ceramic processing described previously [8]. The samples were identified by X-ray powder diffraction as single, perovskite-like phases. The changes in the oxygen non-stoichiometry, which depend on the partial pressure of oxygen in equilibrium with the specimens at different temperatures, were measured by coulometric titration technique as described elsewhere [9]. The absolute values of oxygen content in as-prepared samples were found from reduction in a Setaram TG-DTA-92 thermoanalyzer using a 5% H_2 :95% Ar gas mixture and from the results of chromatometric titration [10]. Within experimental errors both methods gave the same values of δ . The absolute values of the oxygen non-stoichiometry were used as reference data in the coulometric titration measurements.

Ceramic samples with densities of about 93% of the theoretical were obtained by sintering uniaxially pressed powders at 1200–1400°C in air. The specimens were annealed at the sintering temperature for 20 h and then slowly cooled to room temperature. Then, rectangular bars $2 \times 2 \times 18$ mm were cut from the ceramic samples and used for electrical measurements.

The electrical conductivity and thermopower were measured in a special cell described previously [11]. The platinum legs of Pt-Pt10Rh thermocouples were attached to the butt ends of the specimen and served as current leads or voltage probes in measurements of conductivity or thermopower, respectively. Two additional voltage probes for four-point d.c. conductivity measurements were made of Pt wire and wound on the sample with a 10-mm spacing. The measuring cell was made of cubically stabilized zirconia. Two pairs of platinum electrodes were deposited on inner and outer sides of the cell and served as oxygen electrochemical pump and the sensor. The cell with the wired specimen was evacuated and filled with the gas mixture containing 50% O_2 and 50% CO_2 in the beginning of the measurements. The cell enabled independent setting and control of the oxygen partial pressure ($p\text{O}_2$) around the specimen via computer control of the pump and sensor. The electrical parameters were measured with a high-precision voltmeter Solartron 7081. The temperature gradient of about 10°/cm was used for the thermopower measurements. The electrical conductivity was measured in the “true- Ω ” regime, avoiding the influence of the thermal e.m.f. on the measured values. The values of conductivity and thermopower were collected upon achievement of equilibrium between the sample and oxygen gas in the ambient. The criteria for reaching equilibrium were selected changes in logarithm of the conductivity less than 0.01% per minute and changes in thermopower less than 0.001 $\mu\text{V}/\text{min}$ under a fixed oxygen pressure inside the cell. The measurements were carried out in isothermal runs. The relaxation time for σ and S varied from several dozen minutes to several hours during transition from one equilibrium $p\text{O}_2$ value to another, depending on temperature, oxygen partial pressure and cation composition. The above-described criteria are believed to ensure that obtained conductivity and thermopower data obtained in these experiments correspond to equilibrium oxygen contents. Upon achievement of the desirable low oxygen pressure limit, the measurement were halted and then the oxygen pressure was increased to the starting upper limit, where the measurements were repeated in order to confirm reversibility of the experiment. Thereupon temperature was changed thus enabling the next measuring cycle. Thermopower data were corrected for the contribution of the platinum leads [12].

3. Results

The experimental values of oxygen content in $\text{La}_{0.7}\text{Sr}_{0.3}\text{Co}_{1-z}\text{Mn}_z\text{O}_{3-\delta}$ ($z = 0$ and 0.25) are shown as a function of $\log(p\text{O}_2)$ at different temperatures in Fig. 1. These data contain significant information concerning defects and their interactions in non-stoichiometric oxides [13]. For instance, the partial enthalpy of the crystal lattice oxygen relative to the gas phase oxygen can be calculated as $\Delta H_{\text{O}} = (R/2)[\partial \ln(p\text{O}_2)/\partial(1/T)]$. The respective plot vs. oxygen content is presented for $\text{La}_{0.7}\text{Sr}_{0.3}\text{CoO}_{3-\delta}$ in Fig. 2 along with available literature data for comparison. The partial enthalpy substantially decreases with oxygen content, i.e. with the increase in oxygen vacancy concentration. In other words, oxygen vacancies in the cobaltite cannot be regarded as an ideal ensemble where the partial enthalpy must be independent on concentration of constituent species. The deviations of thermodynamic functions from the laws of an ideal solution reflect defect interactions in complex oxides. Such interactions may result in formation of vacancy associates, defect agglomerates and other extended defects. As shown by van Roosmalen and Cordfunke [6] clusters that incorporate localized electrons and oxygen vacancies are quite typical in perovskite-like oxides. More detailed analysis of thermodynamic

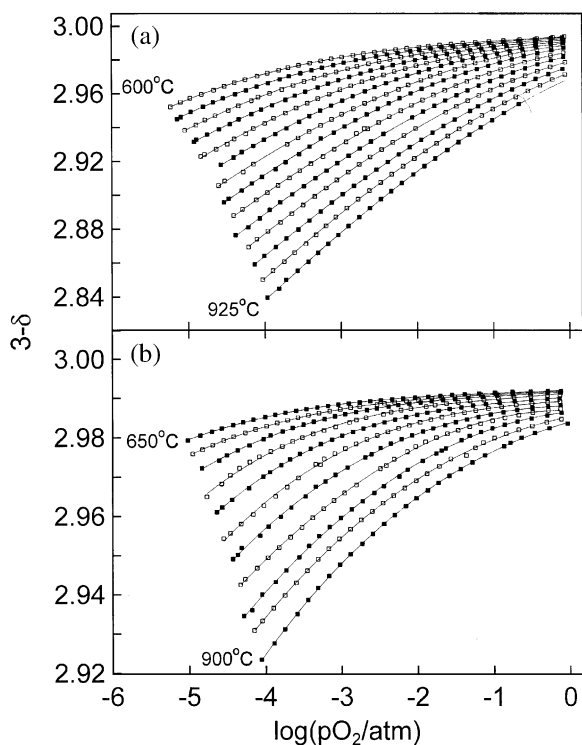


Fig. 1. The equilibrium oxygen content in $\text{La}_{0.7}\text{Sr}_{0.3}\text{CoO}_{3-\delta}$ (a) and $\text{La}_{0.7}\text{Sr}_{0.3}\text{Co}_{0.75}\text{Mn}_{0.25}\text{O}_{3-\delta}$ (b) vs. the logarithm of the oxygen partial pressure at different temperatures. The temperature step between isotherms is to 25°C . Solid lines serve as the guide to an eye.

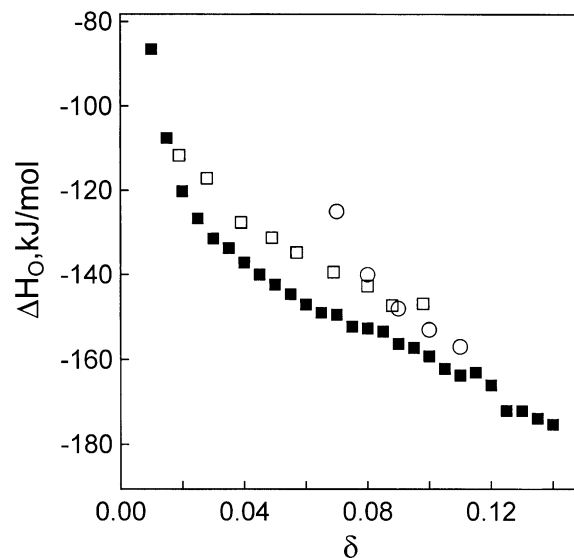


Fig. 2. The partial molar enthalpy of oxygen depending on oxygen non-stoichiometry in $\text{La}_{0.7}\text{Sr}_{0.3}\text{CoO}_{3-\delta}$ (■). The data obtained in Refs. [4,5] are shown for comparison with symbols (□) and (○), respectively.

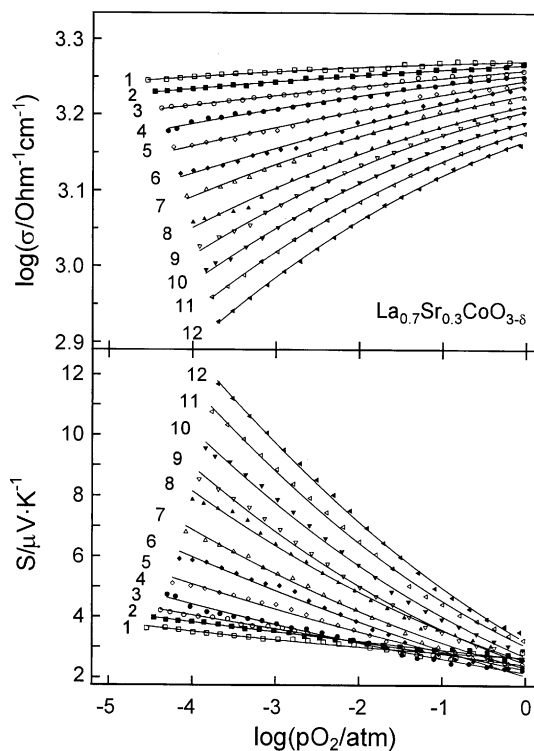


Fig. 3. The logarithm of the conductivity and thermopower in $\text{La}_{0.7}\text{Sr}_{0.3}\text{CoO}_{3-\delta}$ depending on the logarithm of oxygen partial pressure at different temperatures: (1) 650°C , (2) 675°C , (3) 700°C , (4) 725°C , (5) 750°C , (6) 775°C , (7) 800°C , (8) 825°C , (9) 850°C , (10) 875°C , (11) 900°C , (12) 925°C . Solid lines serve as the guide to an eye.

properties will be given elsewhere [14]. The measured data for electrical conductivity and thermopower are shown in Figs. 3 and 4. In combination with data in Fig. 1, the electric properties at selected values of oxygen

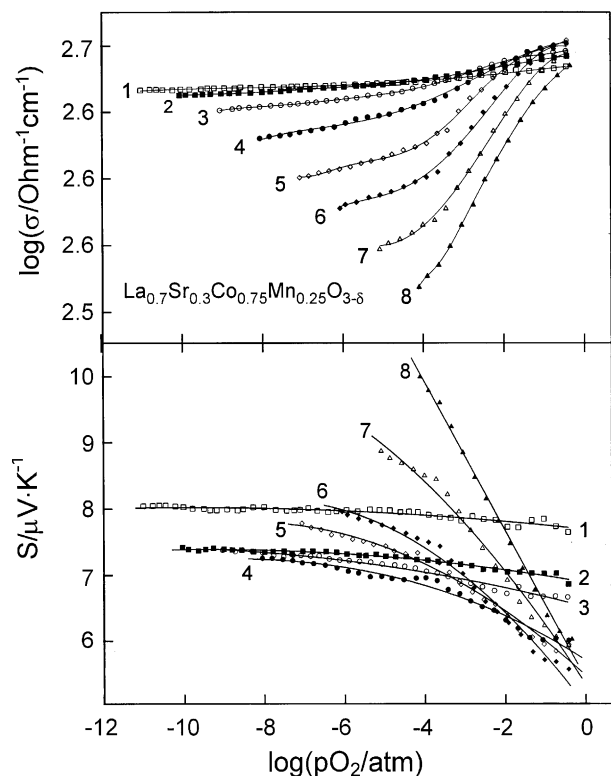


Fig. 4. The logarithm of the conductivity and thermopower in $\text{La}_{0.7}\text{Sr}_{0.3}\text{Co}_{0.75}\text{Mn}_{0.25}\text{O}_{3-\delta}$ depending on the logarithm of oxygen partial pressure at different temperatures: (1) 600°C, (2) 650°C, (3) 700°C, (4) 750°C, (5) 800°C, (6) 850°C, (7) 900°C, (8) 950°C. Solid lines serve as the guide to an eye.

non-stoichiometry are plotted as a function of temperature, Figs. 5 and 6.

A number of observations can be made from the plots in Figs. 5 and 6. The electronic conductivity in $\text{La}_{0.7}\text{Sr}_{0.3}\text{CoO}_{3-\delta}$ decreases with temperature as in a metal-like conductor. However, the slope of the conductivity isoconcentrates changes slightly with the increase in oxygen vacancy concentration. This feature is difficult to explain within a broadband conduction model where an increase in concentration of scattering centers (oxygen vacancies) may result in the conductivity decrease but should not change the slope of the conductivity vs. temperature plots. The thermopower generally increases with temperature also like in a metal. Still, the high-temperature-dependent behavior of the thermopower isoconcentrate at small oxygen deficiency, $\delta = 0.03$, is characteristic of a semiconductor. The partial replacement of cobalt for manganese and increase in oxygen deficiency both result in a decrease of conductivity being of metal type. These variations suggest that the concentration of charge carriers in $\text{La}_{0.7}\text{Sr}_{0.3}\text{Co}_{0.75}\text{Mn}_{0.25}\text{O}_{3-\delta}$ decreased compared to the cobaltite $\text{La}_{0.7}\text{Sr}_{0.3}\text{CoO}_{3-\delta}$. In general, the cobaltites may manifest characteristics in the high-temperature range of either a metal or a semiconductor depending on

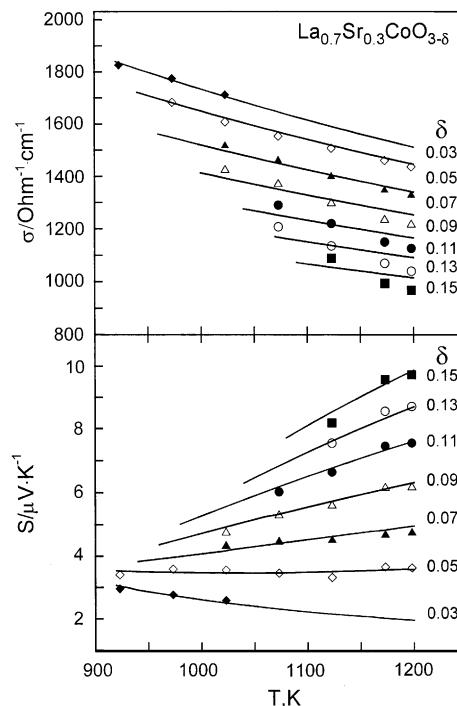


Fig. 5. The temperature dependencies of conductivity and thermopower in $\text{La}_{0.7}\text{Sr}_{0.3}\text{CoO}_{3-\delta}$ at different values of oxygen non-stoichiometry. Solid lines show the calculation results.

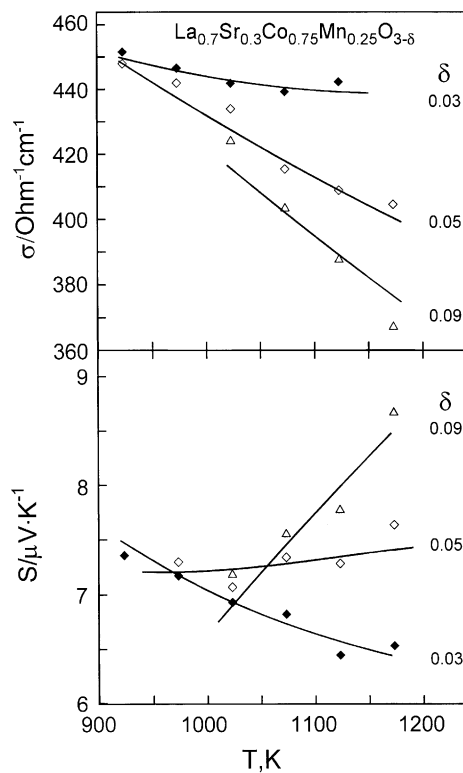


Fig. 6. The temperature dependencies of conductivity and thermopower in $\text{La}_{0.7}\text{Sr}_{0.3}\text{Co}_{0.75}\text{Mn}_{0.25}\text{O}_{3-\delta}$ at different values of oxygen non-stoichiometry. Solid lines show the calculation results.

oxygen content, and it is, therefore, important to decide what picture should be used to interpret the obtained data. One can note in this relation that arguments are known in support of basically a metal-like nature of cobaltites. Thus, valence band photoelectron spectra [15] for $\text{La}_{1-x}\text{Sr}_x\text{CoO}_3$, $x \leq 0.5$, may be interpreted in terms of a band model. More recent analysis of the high-temperature redox thermodynamics supports itinerant behavior of the electronic charge carriers in $\text{La}_{1-x}\text{Sr}_x\text{CoO}_{3-\delta}$, $0.2 \leq x \leq 0.7$ [16]. The high electrical conductivity in the lanthanum cobaltite and its doped derivatives is also often used as evidence for broadband conduction. It is argued, however, by Sehlin et al. [1] that such values are not inconsistent with a narrow band, small polaron-type conduction mechanism provided that a significant fraction of the conduction sites contain charge carriers. Moreover, quite a few works are known where low-temperature electron transport and magnetic properties of cobaltites are discussed under assumption of a localized nature of electronic carriers [17]. With these arguments in mind and considering the data obtained in the high-temperature range, Figs. 5 and 6, it seems that the anomalous features in the electron transport such as the drastic changes in the temperature behavior of thermopower with minute variations in oxygen content and more robust metal-like behavior of conductivity are difficult to reconcile within a broadband conduction mechanism. An alternative and perhaps more plausible explanation may be a small polaron conduction mechanism that takes into account the temperature-dependent reactions of charge disproportionation of the cobalt ions and trapping of polaronic carriers on defects within the crystal structure such as oxygen vacancies and dopants.

4. Model and discussion

Based upon the results of previous studies of lanthanum cobaltite and related oxides, the mechanism of disproportionation is considered to be the primary intrinsic charge carrier formation reaction

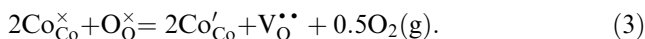


leading to appearance of the p- and n-type carriers, or $\text{Co}_{\text{Co}}^{\bullet}$ and Co'_{Co} in quasi-chemical notations, in place of some amount of the quasi-neutral metal sites, $\text{Co}_{\text{Co}}^{\times}$. Additional, extrinsic p-type carriers appear in response to acceptor doping, e.g. partial replacement of lanthanum for strontium



while oxygen vacancies, $\text{V}_{\text{O}}^{\bullet}$, appearing in the crystal lattice because of the changes in environment, are assumed to be charge compensated by extrinsic n-type

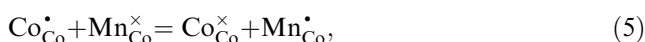
carriers



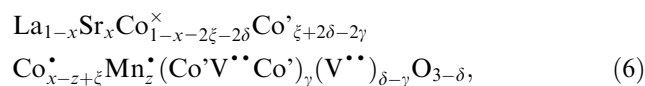
It is possible that some amount of n-type carriers and oxygen vacancies may form quasi-neutral associates $(\text{Co}'_{\text{Co}}\text{V}_{\text{O}}^{\bullet}\text{Co}'_{\text{Co}})$ [6] wherein n-type carriers are assumed to be strongly localized so that they do not participate in the conduction process. The equilibrium of the associates and their constituent species corresponds to the reaction



The partial replacement of cobalt for manganese as $\text{Mn}_{\text{Co}}^{\bullet}(t_{2g}^3)$ is believed to result in strong localization of holes [18,19]



i.e., in immobilization of the respective amount of holes on manganese sites. Applying structure conservation and charge neutrality requirements results in the following formula for the doped cobaltite



where subscripts designating locations of the species are omitted for brevity. Though lengthy, this formula enables one to easily visualize concentrations of different species appearing in the oxide in response to reactions (1)–(5). We may note here that the charge neutrality requirement $[\text{Co}^{\bullet}] = x - 2\delta$ is often used in the literature to interrelate the concentration of holes and oxygen deficiency in acceptor-doped cobaltites, $\text{La}_{1-x}\text{M}_x\text{CoO}_{3-\delta}$. Such a relation, however, is in a sharp disagreement with the well-known fact that no singular behavior in properties is observed at approaching $\delta = x/2$. It is seen from (6) that the concentration of holes is suggested to depend on oxygen content only indirectly via a shift in the equilibrium of reactions (1)–(5) with a change in the oxygen content. Because of the involvement of several reactions in the equilibrium, and in accord with general principles of thermodynamics, one may expect that the concentration of holes should decrease in a regular manner with the increase of the oxygen deficiency in the cobaltites under study. Note that associated oxygen vacancies may be considered either as included in simplest, minimal clusters $(\text{Co}'_{\text{Co}}\text{V}_{\text{O}}^{\bullet}\text{Co}'_{\text{Co}})$ having concentration γ per formula unit or included in larger, condensed clusters $(\text{Co}'_{\text{Co}}\text{V}_{\text{O}}^{\bullet}\text{Co}'_{\text{Co}})_m$ having concentration γ/m per formula unit. Therefore, although formula (6) shows only the amount of the n-type carriers trapped within clusters (and of p-type carriers trapped on Mn species), it is consistent with a spectrum of associates in the solid.

The conduction process is thought to develop in the oxide primarily as a result of charge transfer from a

$\text{Co}_{\text{Co}}^{\bullet}$ or $\text{Co}_{\text{Co}}^{\prime}$ site to a neighboring $\text{Co}_{\text{Co}}^{\times}$ site, i.e., as jumps of p- and n-type carriers, respectively, over available sites. Assuming the dilute limit, where activities of the various ion species can be equated with their respective concentrations, the equilibrium conditions for reactions (1) and (4) can be written as

$$\frac{[\text{Co}_{\text{Co}}^{\bullet}][\text{Co}_{\text{Co}}^{\prime}]}{[\text{Co}_{\text{Co}}^{\times}]^2} = \frac{(x - z + \xi)(\xi + 2\delta - 2\gamma)}{(1 - x - 2\xi - 2\delta)^2} = \exp\left(-\frac{\Delta G_d}{kT}\right), \quad (7)$$

$$\frac{[\text{Co}_{\text{Co}}^{\prime}]^2[\text{V}_{\text{O}}^{\bullet\bullet}]}{[(\text{Co}_{\text{Co}}^{\prime}\text{V}_{\text{O}}^{\bullet\bullet}\text{Co}_{\text{Co}}^{\prime})]} = \frac{(\xi + 2\delta - 2\gamma)^2(\delta - \gamma)}{\gamma} = \exp\left(-\frac{\Delta G_a}{kT}\right), \quad (8)$$

where k is the Boltzmann constant and ΔG_d and ΔG_a are changes in free energies associated with reactions (1) and (4), respectively. In systems containing large concentrations of charge carriers the dilute limit may not be valid. In order to account for deviations from the dilute limit, Sehlin et al. [1] suggested to use the disproportionation free energy change in the form

$$\Delta G_d = \Delta G_0 - \Delta G_1 c_p^{1/3}, \quad (9)$$

where ΔG_0 and ΔG_1 are constants and c_p is the sum of the charge carrier fraction arising from the disproportionation reaction and the charge carrier fraction arising from extrinsic sources. The origin of the second term in Eq. (9) is related to the Coulomb interaction of charge carriers, which is believed to lower the disproportionation energy ΔG_0 by a factor of $1/r$, where r is the mean separation between carriers. To first order $1/r$ is proportional to $c_p^{1/3}$. The negative sign before ΔG_1 corresponds to the energy decrease. One may expect from this expansion that the second term must be smaller than the first one, i.e. $\Delta G_1 < \Delta G_0$. Also, the order of magnitude for ΔG_d and ΔG_1 may be nearly 0.1 eV because it is a characteristic energy scale for the onset of the temperature driven transition to metal-like state in cobaltites [20]. The association energy ΔG_a may possibly achieve several 10ths of eV because NMR experiments on cobaltites give evidence to ample amount of the associated vacancies even on heating to above 1000 K [7].

Heikes relations [21] describe the partial contributions to thermopower of n- and p-type carriers in a hopping conductor

$$S_n = -\frac{k}{e} \ln \left\{ \beta_n \frac{1 - c_n}{c_n} \right\}, \quad (10)$$

$$S_p = +\frac{k}{e} \ln \left\{ \frac{1}{\beta_p} \frac{1 - c_p}{c_p} \right\}, \quad (11)$$

where e is absolute value of the electron charge. The respective fractional concentrations of n- and p-type carriers are

$$c_n = \frac{[\text{Co}_{\text{Co}}^{\prime}]}{[\text{Co}_{\text{Co}}^{\times}] + [\text{Co}_{\text{Co}}^{\prime}]} = \frac{\xi + 2\delta - 2\gamma}{1 - x - \xi - 2\gamma}, \quad (12)$$

$$c_p = \frac{[\text{Co}_{\text{Co}}^{\bullet}]}{[\text{Co}_{\text{Co}}^{\times}] + [\text{Co}_{\text{Co}}^{\bullet}]} = \frac{x - z + \xi}{1 - z - \xi - 2\delta}. \quad (13)$$

The spin degeneracy factors [21] can be accepted as $\beta_p = \frac{5}{6}$ and $\beta_n = \frac{4}{5}$ assuming that the cobalt cations are in their respective high-spin configurations. Note here that the dependence on temperature of the parameters ξ and γ , which follows from Eqs. (7) and (8), may result in variations with temperature of the fractional concentrations and, therefore, of the partial contributions to thermopower, Eqs. (10) and (11). The partial contributions can be utilized to calculate the overall thermopower with the using of the known relation

$$S = \frac{A S_n c_n + S_p c_p}{A c_n + c_p}. \quad (14)$$

The mobility ratio A in Eq. (14) is defined as $A = \mu_n/\mu_p = A_0 \exp(-\Delta E/kT)$, where A_0 is a constant and ΔE is the activation energy for n-type mobility minus that for p-type mobility [1]. The characteristic frequencies of the jump attempts that determine the mobility pre-exponents must be nearly equal for n- and p-polarons because these frequencies are mainly defined by the geometry of the perovskite-like crystalline lattice. The value for A_0 is, therefore, expected to be of the order of unity. On the other hand, the energy barrier for the hops of n-type polarons should be somewhat larger than for the hops of p-type polarons because of the size difference of the involved cobalt species. One may expect from this consideration that the transport at high temperatures $\sim 10^3$ K may occur and be sensitive to movement of n-type polarons when ΔE is nearly 0.1 eV or smaller. For larger differences in the mobility activation energy for n- and p-type carriers, the contribution from n-type carriers is so small that only p-type carriers are to be considered.

The temperature dependence for variables ξ and γ at given x , z and δ can be numerically simulated from Eqs. (7) and (8) supposing some starting values for the parameters ΔG_a , ΔG_0 , ΔG_1 . The results at this stage must be consistent with the requirements $0 \leq 2\xi \leq 1 - x - 2\delta$ and $0 \leq \gamma \leq \delta$ that follow from formula (6). The calculated ξ and γ are then used together with the guess values for A_0 and ΔE in order to calculate the temperature dependence of thermopower according to Eq. (14) at any given x , z and δ . The fitting criterion $\sum_{i,j} \{S_{\text{exp}}(T_i, \delta_j) - S_{\text{calc}}(T_i, \delta_j)\}^2 \rightarrow \min$ was used in this work in order to compare the experimental S_{exp} and the calculated S_{calc} values of thermopower. The temperature step was 1 K in the calculations while values of δ

corresponded to those in Fig. 5 or Fig. 6. In principle, there may be several minima in the five-dimensional space of the minimization task. However, correct parameters must have physically reasonable values and, moreover, further calculations of the mobility of the carriers from the conductivity must also result in meaningful values for the mobility activation energy.

Reasonable fits to the temperature dependencies of the thermopower isoconcentrates for $\text{La}_{0.7}\text{Sr}_{0.3}\text{CoO}_{3-\delta}$ ($z = 0$) in Fig. 5 are obtained using the following parameters values: $\Delta G_0 = 0.125$ eV, $\Delta G_1 = 0.075$ eV, $\Delta G_a = 0.32$ eV and $\Delta E = 0.03$ eV. The values of A_0 are found equal to 0.96, 1.07, 1.19, 1.33, 1.49, 1.70 and 1.94 at δ 's equal to 0.03, 0.05, 0.07, 0.09, 0.11, 0.13 and 0.15, respectively. These changes in A_0 are expected because increasing the removal of oxygen ions, which themselves are key intermediates in hole jumps, from the crystal lattice renders jumps increasingly less frequent from one cobalt cation to the neighboring one. Similarly, an increase of δ in the partially substituted specimen $\text{La}_{0.7}\text{Sr}_{0.3}\text{Co}_{0.75}\text{Mn}_{0.25}\text{O}_{3-\delta}$ ($z = 0.25$) results in an increase of the parameter A_0 . Moreover, the value of A_0 at a given value of δ becomes somewhat larger with manganese substitution. For instance, values of A_0 at $\delta = 0.09$ are equal to 1.33 and 1.59 in $\text{La}_{0.7}\text{Sr}_{0.3}\text{CoO}_{3-\delta}$ and $\text{La}_{0.7}\text{Sr}_{0.3}\text{Co}_{0.75}\text{Mn}_{0.25}\text{O}_{3-\delta}$, respectively. These results indicate that manganese cations serve not only to trap hole, but also exert an additional influence on the frequency of jumps of holes over cobalt cations. Such an influence is not surprising because manganese doping results in local deformations of the cobalt–oxygen network. At the same time, values of the other parameters, i.e. ΔG_0 , ΔG_1 , ΔG_a and ΔE , in $\text{La}_{0.7}\text{Sr}_{0.3}\text{Co}_{0.75}\text{Mn}_{0.25}\text{O}_{3-\delta}$ are found to remain essentially the same as in $\text{La}_{0.7}\text{Sr}_{0.3}\text{CoO}_{3-\delta}$ for acceptable fitting of the calculated results to the experimental thermopower data, Fig. 6. The screened charge disproportionation energy ΔG_d generated by the model is found equal to about 0.06 eV for both $\text{La}_{0.7}\text{Sr}_{0.3}\text{CoO}_{3-\delta}$ and $\text{La}_{0.7}\text{Sr}_{0.3}\text{Co}_{0.75}\text{Mn}_{0.25}\text{O}_{3-\delta}$. This value is of the same order of magnitude in $\text{La}_{1-x}\text{Ca}_x\text{CoO}_3$ at elevated temperatures. Also, ΔG_d decreases slowly with the temperature increase in the studied temperature range, which again is in accord with the high-temperature behavior of the disproportionation energy in the calcium-doped cobaltite [1]. The thermodynamic analysis [14] of the equilibrium diagrams in Fig. 1, which involves the disorder reactions (1)–(5), results in the vacancy association energy ΔG_a equal to about 0.3 eV, a value that is in favorable correspondence with the estimation $\Delta G_a = 0.32$ eV obtained from the thermopower fits. Note also that the results can be made to follow the experimental data more closely when strontium and manganese concentrations are allowed to vary, i.e., when they are considered as free parameters. In such case, the calculated values of x

and z tend to be smaller to about 20–30% than their nominal values $x = 0.3$ and $z = 0.25$. A similar trend was observed before in the study [22] of the $(\text{La}, \text{Ca})(\text{Co}, \text{Cr})\text{O}_3$ series, where it was supposed to be related with oxygen deficiency. Alternatively, these results may possibly be interpreted as an indication that the admixture cations in the parent oxide LaCoO_3 are not evenly distributed. Indeed, it is well known in the physics of semiconductors [23] that clustering of dopants results in a decrease of their ionization degree. Hence, the amount of extrinsic holes may be smaller than the nominal concentration of acceptors because a perfectly even distribution of admixtures over the crystal, when all of them are located far from each other, is difficult to achieve even under the most thorough preparation conditions. This is particularly so when the concentration of admixture cations is large as is the case in this study. Moreover, it is important to remember that a number of other simplifications are made in the model, such as neglecting a population of the low- and intermediate-spin cobalt species, crystal lattice relaxation in response to introduction of oxygen vacancies, strontium and manganese, disregarding of the hole jumps involving manganese cations, etc. Keeping these factors in mind and considering that the thermopower fits are rather satisfactory over the entire temperature range studied and at all available values of oxygen non-stoichiometry, the polaron model of the electronic transport, which is based on disorder reactions (1)–(5) and Eqs. (7)–(14), can be viewed as a reasonably correct description of the conduction process at high temperatures in the moderately doped oxide $\text{La}_{0.7}\text{Sr}_{0.3}\text{Co}_{0.75}\text{Mn}_{0.25}\text{O}_{3-\delta}$.

The intrinsic electron/hole population ξ , which arises as a result of charge disproportionation, slowly increases with temperature, while the concentration of vacancy associates γ decreases, see Figs. 7 and 8. These features are both consistent with the temperature-activated character of the charge disproportionation and vacancy association reactions. It can be seen from Figs. 7 and 8 that a substantial part of the oxygen vacancies reside in metal-vacancy clusters even at rather high temperatures. Such persistent clustering of oxygen vacancies is quite common in perovskite and perovskite-related structures, a conclusion corroborated by in situ high-temperature NMR studies [7]. The increase in the total amount of oxygen vacancies δ at a constant temperature results quite naturally in the respective increase of the amount of associated vacancies. At the same time, the amount of electron/hole carriers generated by the disproportionation reaction becomes smaller. Hence, the increase in the oxide ion vacancy concentration favors the increased stability of cobalt species in 3+ oxidation state. This behavior may be related to an enhancement of the ionicity of metal–oxygen chemical bonds with the increase in oxygen vacancy concentration. From the

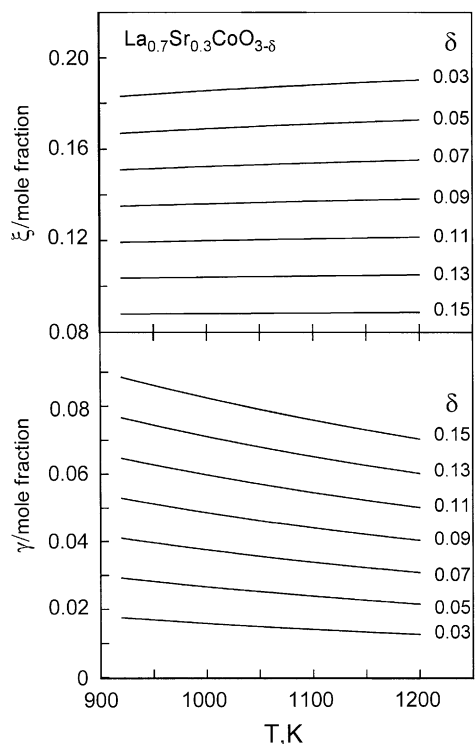


Fig. 7. The calculated dependencies from temperature of charge disproportionation and vacancy association degree at different values of oxygen non-stoichiometry in $\text{La}_{0.7}\text{Sr}_{0.3}\text{CoO}_{3-\delta}$.

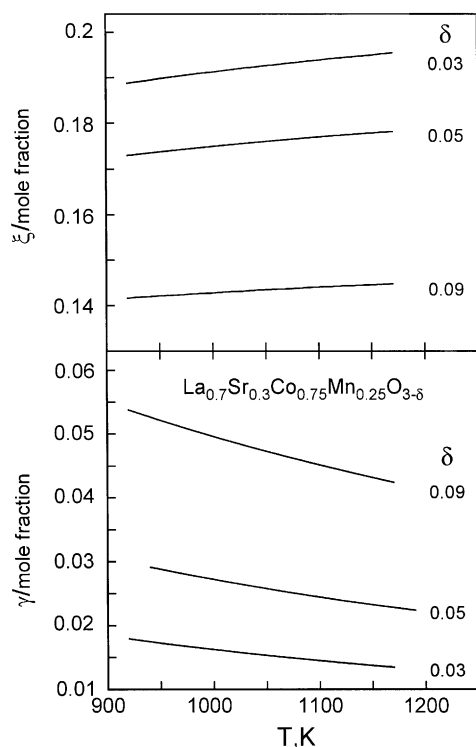


Fig. 8. The calculated dependencies from temperature of charge disproportionation and vacancy association degree at different values of oxygen non-stoichiometry in $\text{La}_{0.7}\text{Sr}_{0.3}\text{Co}_{0.75}\text{Mn}_{0.25}\text{O}_{3-\delta}$.

above discussion, it can be seen that all the mechanisms of electronic compensation, charge trapping and movement occur simultaneously, while their relative contribution to thermopower varies not with temperature only, but with changes in oxygen vacancy concentration and manganese content, thus resulting either in metal- or semiconductor-like variations of thermopower with temperature.

The total electrical conductivity can be calculated [1] as the sum of n- and p-type contributions according to
$$\sigma = \sigma_n + \sigma_p = N\mu_p(c_p + Ac_n). \quad (15)$$

Here, N is a normalization constant, which can be determined by equating the model to the measured electrical conductivity of the corresponding sample at some selected temperature, and $\mu_p \propto ((1 - c_p)/T)\exp(-\varepsilon_p/kT)$ is the temperature-activated mobility of hole carriers. The activation energy ε_p of about 0.03 and 0.06 eV for the hopping of p-type carriers was chosen to produce agreement with the experimental results for conductivity at different values of δ in $\text{La}_{0.7}\text{Sr}_{0.3}\text{CoO}_{3-\delta}$ and $\text{La}_{0.7}\text{Sr}_{0.3}\text{Co}_{0.75}\text{Mn}_{0.25}\text{O}_{3-\delta}$, respectively, Figs. 5 and 6. The calculated mobility activation energy for p-type carriers in $\text{La}_{0.7}\text{Sr}_{0.3}\text{CoO}_{3-\delta}$ is in favorable comparison with the value of 0.044 eV for the p-type mobility in $\text{La}_{0.7}\text{Ca}_{0.2}\text{CoO}_3$. The difference may be a result of the larger level of acceptor doping [1]. It is interesting to note also that the hopping energy that follows from the high-temperature data has the same order as that obtained from the a.c. conductivity measurements on $\text{La}_{1-x}\text{Sr}_x\text{CoO}_3$ in the low-temperature range [17]. The activation energies for the hops of n-type polarons in $\text{La}_{0.7}\text{Sr}_{0.3}\text{CoO}_{3-\delta}$ and $\text{La}_{0.7}\text{Sr}_{0.3}\text{Co}_{0.75}\text{Mn}_{0.25}\text{O}_{3-\delta}$ can be evaluated from the obtained difference ΔE in the activation energy for mobility of n- and p-type carriers equal to about 0.06 and 0.09 eV, respectively.

5. Conclusions

The measurements of equilibrium oxygen content, electrical conductivity and thermopower have been carried out in the perovskite-like oxides $\text{La}_{0.7}\text{Sr}_{0.3}\text{Co}_{1-z}\text{Mn}_z\text{O}_{3-\delta}$ ($z = 0$ and 0.25). The obtained variations in oxygen content with oxygen partial pressure and temperature are utilized to find temperature dependencies of conductivity and thermopower in $\text{La}_{0.7}\text{Sr}_{0.3}\text{Co}_{1-z}\text{Mn}_z\text{O}_{3-\delta}$ at different values of the non-stoichiometry. The temperature dependencies of the thermopower in $\text{La}_{0.7}\text{Sr}_{0.3}\text{CoO}_{3-\delta}$ are modeled using known expression for thermopower in a hopping conductor, the screened charge disproportionation mechanism for producing intrinsic n- and p-type carriers and the vacancy association reaction for partial trapping of n-type carriers. The model is extended to the manganese-doped composition $\text{La}_{0.7}\text{Sr}_{0.3}\text{Co}_{0.75}\text{Mn}_{0.25}\text{O}_{3-\delta}$ under the

assumption that the manganese cations act as traps for hole carriers. The variations in oxygen vacancy concentration and manganese content are found to mainly alter the ratio of n-type to p-type mobility. At the same time, energetic parameters governing charge disproportionation of trivalent cobalt cations and formation of vacancy associates are shown to be essentially invariable, which demonstrates that local cobalt–oxygen interactions are not changed quantitatively at moderate disturbance of the cobalt–oxygen network. However, the relative amount of labile and trapped, n- and p-type charge carriers depends on total oxygen vacancy concentration and temperature thus resulting in either semiconductor- or metal-like temperature changes of thermopower. The model parameters chosen to fit thermopower also give a qualitative fit to the electrical conductivity data, assuming an expression for the temperature dependence of the mobility based upon a small polaron conduction mechanism.

Acknowledgments

This research was supported by the International Association (INTAS) of the European Community under Contract No. 2000-00728. The partial support from the US Civilian Research and Development Foundation (CRDF, Grant No. REC 005) is greatly appreciated. One of us (K.R.P.) is grateful to the EMSI program of the National Science Foundation and the US Department of Energy Office of Science (CHE-9810378) at the Northwestern University Institute for Environmental Catalysis. We are particularly grateful to the reviewer who attracted our attention to publication [17].

References

- [1] S.R. Sehlin, H.U. Anderson, D.M. Sparlin, *Phys. Rev. B* 52 (1995) 11681–11689.
- [2] V.A. Cherepanov, L.Ya. Gavrilova, O.A. Bukhner, in: J. Routbort, R. Dickman, T. Mason (Eds.), *Abstr. Eng. Found. Conf. Nonstoichiometric Ceramics and Intermetallics*, April 26–May 1, Kona, Hawaii, 1998, p. 96.
- [3] J. Mizusaki, J. Tabuchi, T. Matsuura, S. Yamauchi, K. Fueki, *J. Electrochem. Soc.* 136 (1989) 2082–2088.
- [4] J. Mizusaki, Y. Mima, S. Yamauchi, K. Fueki, H. Tagawa, *J. Solid State Chem.* 80 (1989) 102–111.
- [5] A.N. Petrov, V.A. Cherepanov, O.F. Kononchuk, L.Ya. Gavrilova, *J. Solid State Chem.* 87 (1990) 69–76.
- [6] J.A.M. van Roosmalen, E.H.P. Cordfunke, *J. Solid State Chem.* 93 (1991) 212–219.
- [7] S. Adler, S. Russek, J. Reimer, M. Fendorf, A. Stacy, Q. Huang, A. Santoro, J. Lynn, J. Baltisberger, U. Werner, *Solid State Ionics* 68 (1994) 193–211.
- [8] A.N. Petrov, V.I. Voronin, T. Norby, P. Kofstad, *J. Solid State Chem.* 143 (1999) 52–57.
- [9] M.V. Patrakeev, E.B. Mitberg, A.A. Lakhtin, I.A. Leonidov, V.L. Kozhevnikov, K.R. Poeppelmeier, *Ionics* 4 (1998) 191–199.
- [10] P. Kofstad, A. Petrov, in: F.W. Poulsen, J.J. Bentzen (Eds.), *Proceedings of the 14th Riso International Symposium on Material Science*, 1993, p. 287.
- [11] M.V. Patrakeev, E.B. Mitberg, I.A. Leonidov, V.L. Kozhevnikov, *Solid State Ionics* 139 (2001) 325–330.
- [12] N. Cusak, P. Kendall, *Proc. Phys. Soc.* 72 (1958) 898–901.
- [13] V.I. Tsidilkovskii, I.A. Leonidov, A.A. Lakhtin, V.A. Mezrin, *Phys. Stat. Sol. B* 168 (1991) 233–244.
- [14] A.N. Petrov, V.L. Kozhevnikov, I.A. Leonidov, M.V. Patrakeev, T. Norby, *Solid State Ionics*, unpublished.
- [15] J.P. Kemp, D.J. Beal, P.A. Cox, *J. Solid State Chem.* 86 (1990) 50–58.
- [16] M.H.R. Lankhorst, H.J.M. Bouwmeester, H. Verweij, *J. Solid State Chem.* 133 (1997) 555–567.
- [17] E. Iguchi, K. Ueda, H. Nakatsugawa, *J. Phys.: Condens. Matter* 10 (1998) 8999–9013 (see also references therein).
- [18] G.H. Jonker, *J. Appl. Phys.* 37 (1966) 1424–1430.
- [19] G.Ch. Kostogloudis, P. Fertis, Ch. Ftikos, *Solid State Ionics* 118 (1999) 241–249.
- [20] P.M. Raccach, J.B. Goodenough, *Phys. Rev.* 155 (1967) 932–943.
- [21] J.-P. Doumerc, *J. Solid State Chem.* 110 (1994) 419–420.
- [22] S.R. Sehlin, H.U. Anderson, D.M. Sparlin, *Solid State Ionics* 78 (1995) 235–244.
- [23] V.L. Bonch-Bruevitch, S.G. Kalashnikov, in: V.A. Dubnova (Ed.), *Physics of Semiconductors*, Nauka Publishing House, Moscow, 1977, p. 672 (in Russian).